Oncogene (2011) 1–13

www.nature.com/onc

ORIGINAL ARTICLE

CD49f and CD61 identify Her2/neu-induced mammary tumor-initiating cells that are potentially derived from luminal progenitors and maintained by the integrin–TGFβ signaling

P-K Lo[1,2,6], D Kanojia[1,2,6], X Liu[3], UP Singh[4], FG Berger[1,2], Q Wang[2,5] and H Chen[1,2]

[1]*Department of Biological Sciences, University of South Carolina, Columbia, SC, USA;* [2]*Center for Colon Cancer Research, University of South Carolina, Columbia, SC, USA;* [3]*Department of Mathematics, University of South Carolina, Columbia, SC, USA;* [4]*Department of Pathology, Microbiology and Immunology, School of Medicine, University of South Carolina, Columbia, SC, USA and* [5]*Department of Chemistry and Biochemistry, University of South Carolina, Columbia, SC, USA*

Human epidermal growth factor receptor 2 (HER2)/Neu is overexpressed in 20–30% of breast cancers and associated with aggressive phenotypes and poor prognosis. For deciphering the role of HER2/Neu in breast cancer, mouse mammary tumor virus (MMTV)-*Her2/neu* transgenic mice that develop mammary tumors resembling human HER2-subtype breast cancer have been established. Several recent studies have revealed that HER2/Neu is overexpressed in and regulates self renewal of breast tumor-initiating cells (TICs). However, in the MMTV-*Her2/neu* transgenic mouse model, the identity of TICs remains elusive, despite previous studies showing supportive evidence for existence of TICs in Her2/neu-induced mammary tumors. Through systematic screening and characterization, we identified that surface markers CD49f, CD61 and ESA were aberrantly overexpressed in Her2-overexpressing mammary tumor cells. Analysis of these markers and CD24 detected anomalous expansion of the luminal progenitor population in preneoplastic mammary glands of *Her2/neu* transgenic mice, indicating that aberrant luminal progenitors originated in Her2-induced mammary tumors. The combined markers, CD49f and CD61, further delineated the CD49f^{high}CD61^{high}-sorted fraction as a TIC-enriched population, which displayed increased tumorsphere formation ability, enhanced tumorigenicity both *in vitro* and *in vivo* and drug resistance to pacitaxel and doxorubicin. Moreover, the TIC-enriched population manifested increased transforming growth factor-β (TGFβ) signaling and exhibited gene expression signatures of stemness, TGFβ signaling and epithelial-to-mesenchymal transition. Our findings that self-renewal and clonogenicity of TICs were suppressed by pharmacologically inhibiting the TGFβ signaling further indicate that the TGFβ pathway is vital for maintenance of the TIC population. Finally, we showed that the integrin-β3 (CD61) signaling pathway was required for sustaining active TGFβ signaling and self-renewal of TICs. We for the first time developed a technique to highly enrich TICs from mammary tumors of *Her2/neu* transgenic mice, unraveled their properties and identified the cooperative integrin-β3–TGFβ signaling axis as a potential therapeutic target for HER2-induced TICs.

Oncogene advance online publication, 26 September 2011; doi:10.1038/onc.2011.439

Keywords: tumor-initiating cells; Her2/neu; mammary tumor; CD49f; CD61; ESA

Introduction

According to the cancer stem cell (CSC) hypothesis, a variety of tumors may be initiated and maintained by a subpopulation of cells that exhibit characteristics of stem cells. In addition to driving carcinogenesis, these CSCs, also called tumor-initiating cells (TICs), may contribute to therapeutic resistance (Clarke *et al*., 2006). Several recent studies have shown that human epidermal growth factor receptor 2 (HER2) may have a role in regulation of the TIC population. First, TICs of HER2-overexpressing breast cancer cell lines express the highest HER2 levels in the bulk cell population (Magnifico *et al*., 2009). Second, overexpression of HER2 in normal mammary epithelial cells increases the proportion of stem/progenitor cells (Korkaya *et al*., 2008). Third, the HER2 inhibitor (trasuzumab or lapitinib) is able to specifically target this HER2-overexpressing TIC population (Korkaya *et al*., 2008; Magnifico *et al*., 2009). Finally, a decrease in TICs was observed in HER2-positive tumors of patients receiving the epidermal growth factor receptor/HER2 inhibitor treatment (Li *et al*., 2008). These lines of evidence suggest that the HER2 signaling drives carcinogenesis through regulation of the mammary stem/progenitor cell population.

The role of Her2/neu in regulating TIC properties was also studied in the mouse mammary tumor virus (MMTV)-*Her2/neu* transgenic mouse model. Liu *et al*., (2007) first functionally identified the existence of TICs

Correspondence: Dr H Chen, Department of Biological Sciences, University of South Carolina, 715 Sumter Street, PSC621, Columbia, SC 29208, USA.
E-mail: hchen@biol.sc.edu
[6]These authors contributed equally to this work.
Received 12 June 2011; revised 21 August 2011; accepted 24 August 2011

in primary mammary tumors of MMTV-*Her2/neu* transgenic mice, and Cicalese *et al*. (2009) showed that the self-renewal division of TICs is more frequent in Her2/neu-induced tumors than normal stem cells in their normal counterparts. Furthermore, the gene profiles of MMTV-*Her2/neu* mammary tumors are most congruent with the gene signature of luminal progenitor cells, suggesting that Her2-induced mammary tumors may be developed from altered mammary luminal progenitor cells (Lim *et al*., 2010). Despite supportive evidence from these studies, currently there are no available methods developed for isolation or enrichment of TICs from Her2/neu-induced mammary tumors. Therefore, although MMTV-*Her2/neu* transgenic mice have been used as a Her2-mediated tumorigenic animal model for about two decades (Guy *et al*., 1992), the identity of TICs in Her2/neu-induced mammary tumors remains largely unknown.

To identify and characterize the putative TICs in the MMTV-*Her2/neu* transgenic mouse model, we screened numerous putative stem/progenitor marker combinations to subdivide the primary mammary tumor cells and their derivative primary cell cultures. By analyzing these markers, we identified luminal progenitors potentially giving rise to Her2-induced TICs. Importantly, we found that the $CD49f^{high}CD61^{high}$ tumor cell subset represents a TIC-enriched population, and the cooperative integrin-β3–transforming growth factor (TGFβ) signaling axis is vital for maintaining Her2-induced TICs. These findings, taken together, suggest that targeting of the cooperative integrin-β3–TGFβ signaling could be developed for the TIC-targeting therapy to treat HER2/Neu-positive breast cancer patients.

Results

Identification of TIC biomarkers for Her2/neu-induced mammary tumors

To identify potential stem cell biomarkers and characterize molecular traits of stemness in Her2-induced mammary tumors, we performed gene expression profiling analysis of 26 putative stem cell markers and 5 epithelial lineage-specific markers (Supplementary Tables 1 and 2) on H6O5 cells derived from Her2-induced mouse primary mammary gland tumors and NMuMG cells, a non-transformed mouse mammary epithelial cell line (Hynes *et al*., 1985) serving as a normal control for comparison. Before gene expression analysis, Her2/neu overexpression in H6O5 cells has been confirmed by western blot analysis and its levels were almost equivalent to those in primary Her2 tumors (Supplementary Figure 1). In all, 9 out of 26 analyzed genes were expressed at higher levels in H6O5 than in NMuMG, including *Abcg2*, *CD49f*, *CD61*, *ESA*, *Nanog*, *Notch3*, *Oct3/4*, *Stat3* and *Tp63* (Supplementary Table 2 and Figure 1a). Among lineage-specific markers, H6O5 cells expressed slightly less mRNA levels of CD24 and the luminal marker *keratin 18* (*Krt18*) and higher levels of myoepithelial markers, such as *Krt5* and *Krt14*, than NMuMG cells (Supplementary Table 2). To further validate that nine aberrantly overexpressed genes identified in H6O5 cells were not attributable to forced *in vitro* culture condition, we performed quantitative reverse transcriptase PCR analysis on two samples each of isolated *in vivo* normal epithelial cells from FVB/N mammary glands and tumor epithelial cells from primary Her2/neu mammary gland tumors. As shown in Figure 1b, eight out of nine genes (except *Stat3*) consistently showed aberrant overexpression in primary Her2/neu mammary tumor epithelial cells compared with age-matched normal FVB/N mammary epithelial cells.

Among these differentially expressed genes, *CD49f* (*integrin-α6*), *CD61* (*integrin-β3*) and *ESA* have been identified and used as *bona fide* markers for the enrichment of normal and CSCs (Stingl *et al*., 2006; Asselin-Labat *et al*., 2007; Vaillant *et al*., 2008; Lim *et al*., 2010). To validate quantitative reverse transcriptase PCR results and evaluate whether these selected markers can be potentially used to identify and enrich TICs, fluorescence-activated cell sorting (FACS) analysis was performed on H6O5 cells and two normal mammary epithelial cell lines (NMuMG and C127) to examine the expression status of selected markers, including CD49f, CD29, CD61, Sca1, CD24 and ESA (EpCAM). CD49f, CD61 and ESA were selected because of their aberrant overexpression in H6O5 cells and primary tumors (Figures 1a and b). CD29 and Sca1 were also chosen, as they have been used as markers to identify normal and neoplastic mammary stem and/or progenitor cells (Welm *et al*., 2003; Shackleton *et al*., 2006; Stingl *et al*., 2006; Asselin-Labat *et al*., 2007). CD24 was included in our study on the basis of the studies by Liu *et al*. (2007), showing that only $CD24^{+}$ Her2/neu tumor cells are tumorigenic. As shown in Figure 1c, CD49f, CD61 and ESA were expressed at higher levels in H6O5 cells than in the control cell lines, consistent with the mRNA expression data (Figure 1a). CD29 and CD24 were almost equivalently expressed between these three cell lines (Figure 1c). Sca1 was highly expressed in C127 cells compared with H6O5 and NMuMG cells (Figure 1c). Overall, these data suggest that CD49f, CD61 and ESA are potential candidates as TIC markers because of their differential expression in Her2/neu-transformed tumor cells compared with non-transformed mammary epithelial cells.

Her2/neu-induced tumors are potentially developed from the luminal progenitor population

MMTV-*Her2/neu* transgenic mice develop undifferentiated adenocarcinomas after a long latency (6–12 months; Guy *et al*., 1992). To identify the origin of Her2-transformed TICs, we examined changes in cellular subsets of preneoplastic mammary glands. The previous study showed that CD24 and CD49f can identify mammary stem cells (mammary repopulating units, MRUs) and progenitor cells (mammary colony-forming cells, Ma-CFCs) (Stingl *et al*., 2006). We reproduced these data as shown in Figure 2a (the top panel). Intriguingly, the progenitor cell population

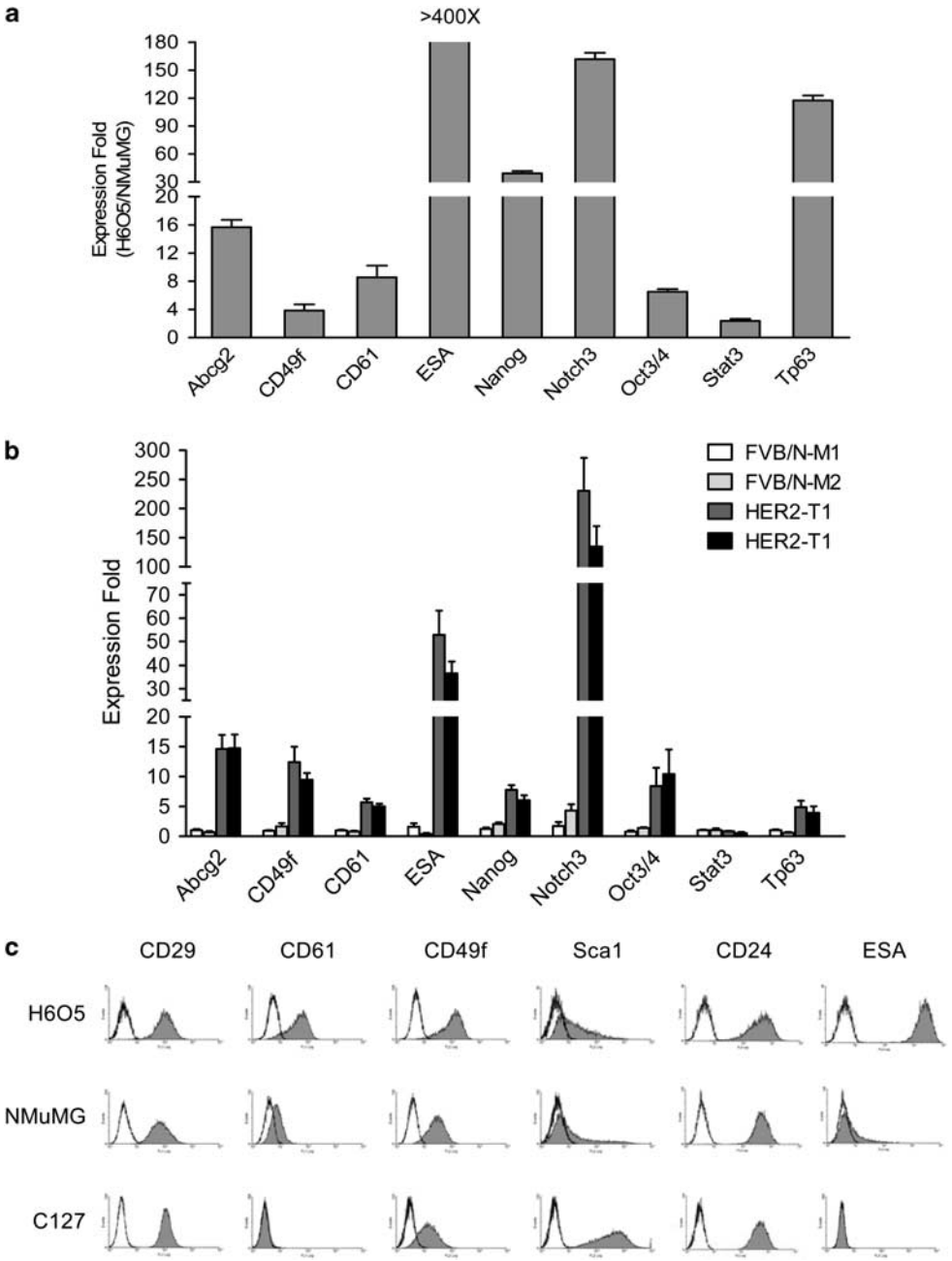

Figure 1 Expression analysis of stem cell marker genes in the tumor cells derived from primary MMTV-*Her2/neu* tumor. (**a**) Quantitative reverse transcriptase PCR (RT–PCR) analysis of stem cell marker genes in H6O5 cells versus NMuMG cells. The mean and s.d. are calculated from triplicate experiments. (**b**) Quantitative expression analysis of stem cell marker genes in normal mammary epithelial cells from FVB/N mice as well as in mammary tumor epithelial cells of primary tumors from *Her2/neu* transgenic mice. Two different complementary DNA samples each for normal or tumor epithelial cells were analyzed by real-time quantitative RT–PCR assays. The expression folds (mean ± s.d.) from triplicate experiments are shown. (**c**) Flow cytometric (FACS) analysis of stem cell surface antigens in H6O5 cells and two immortalized mouse mammary epithelial cell lines, NMuMG and C127. Histograms are shown for displaying distributions of antibody-staining intensities of surface antigens (CD29, CD61, CD49f, Sca1, CD24 and ESA) versus cell numbers.

($Lin^{-}CD24^{high}CD49f^{med/low}$ cells) was aberrantly expanded in preneoplastic mammary glands of MMTV-*Her2/neu* transgenic mice compared with normal counterparts of wild-type FVB/N mice (9.8% vs 3.1%), which overlapped the majority (79.2%) of the primary tumor cell population (Figure 2a). The percentage of the mammary stem cell population ($Lin^{-}CD24^{med}CD49f^{high}$, MRUs) remained unchanged in preneoplastic mammary glands of transgenic mice relative to wild-type mice (0.8% vs 0.7%). We also analyzed the FACS profiles of CD49f and ESA because of the recent findings that these two markers could delineate cellular subsets in human mammary glands (Lim *et al*., 2009). Analogous to the CD24CD49f combination, ESA and CD49f could define

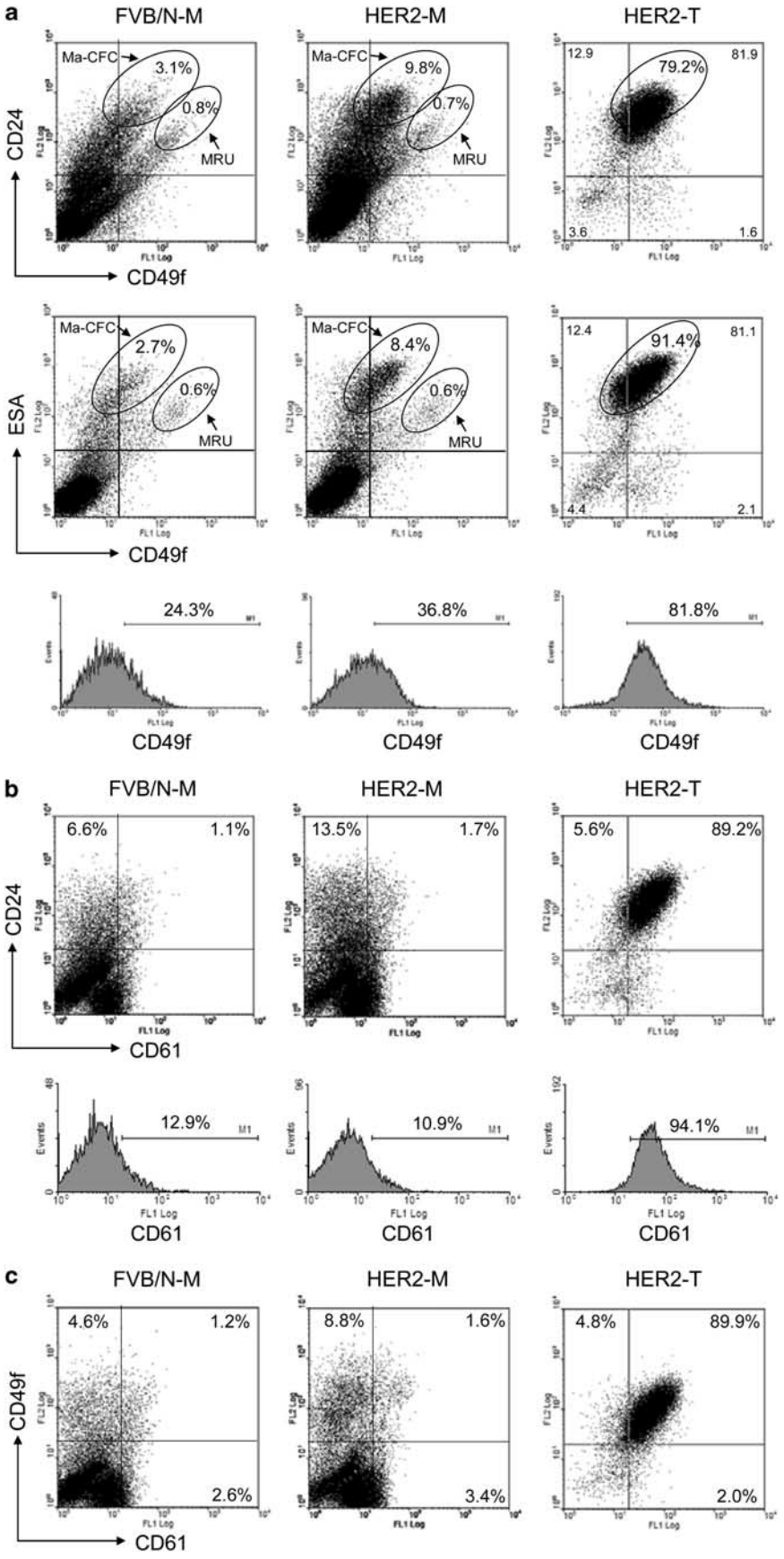
a
FVB/N-M
HER2-M
HER2-T
Ma-CFC
3.1%
0.8%
MRU
9.8%
0.7%
12.9
79.2%
81.9
3.6
1.6
CD24
CD49f
2.7%
0.6%
8.4%
0.6%
12.4
91.4%
81.1
4.4
2.1
ESA
24.3%
36.8%
81.8%
b
6.6%
1.1%
13.5%
1.7%
5.6%
89.2%
CD61
12.9%
10.9%
94.1%
c
4.6%
1.2%
2.6%
8.8%
1.6%
3.4%
4.8%
89.9%
2.0%

the MRU and Ma-CFC populations (Figure 2a, the middle panel). Again, the Lin$^-$ESA^{high}CD49$^{med/low}$ Ma-CFC population, but not the Lin$^-$ESA^{med}CD49f^{high} MRU population, was anomalously expanded in pre-malignant mammary glands of *Her2/neu* transgenic mice (Figure 2a). The FACS patterns showing expansion of the Ma-CFC population in Her2/neu preneoplastic mammary glands (Figure 2a) were reproducible in multiple mice ($n>4$; data not shown). Among Lin$^-$CD24$^+$ mammary epithelial cells, the percentage of Lin$^-$CD49f$^+$ cells progressively increased with tumor development (wild type 24.3%, preneoplastic gland 36.8% and tumor 81.8%; Figure 2a, the bottom panel). According to the studies by Stingl *et al.* (2006), Ma-CFCs preferentially express luminal markers such as *Krt18* and *Krt19*, indicating that they are luminal progenitor cells. We also found that Ma-CFCs exhibited the ESA^{high} profile, a typical luminal feature (Lim *et al.*, 2009). Therefore, our and other lines of evidence, taken together, suggest that the origin of Her2/neu-induced mammary tumor cells is derived from the aberrant luminal progenitor cells.

We also analyzed the cellular subset expressing CD61 in combination with CD24 or CD49f during tumor development in MMTV-*Her2/neu* transgenic mice. Preneoplastic mammary glands exhibited a slight increase in both Lin$^-$CD24$^+$CD61$^+$ (1.7% vs 1.1%) and Lin$^-$CD49f$^+$CD61$^+$ cells (1.6% vs 1.2%) compared with wild-type counterparts, but both Lin$^-$CD24$^+$CD61$^+$ (89.2%) and Lin$^-$CD49f$^+$CD61$^+$ (89.9%) cell populations were drastically expanded in primary tumors (Figures 2b and c). The expansion of Lin$^-$CD24$^+$CD61$^+$ and Lin$^-$CD49f$^+$CD61$^+$ cells in primary tumors was mainly due to a dramatic increase in the Lin$^-$CD61$^+$ cell population, and more importantly there was a significant, tumor-specific increase in the expression level of CD61 at the cellular level. Thus, the transition from preneoplasia to tumor formation is characterized by a significant increase in CD24/ESA/CD49f/CD61-quadruple-positive cells (Figure 2).

The CD49f^{high}CD61^{high} subpopulation exhibits the CD24^{high}ESA^{high} profile and TIC's characteristics

According to the Figure 2 results, we identified CD49f, CD61, ESA and CD24 as potential TIC's makers, as they can be used to track the transformed transition from luminal progenitor cells to Her2-induced tumor cells. To ascertain which two-antigen combination is potential for identifying the TIC population, we performed FACS analysis of five different antigen combinations on *in vitro* cultured H6O5 cells, *in vivo* H6O5-derived xenograft tumors and primary Her2 mammary tumors. As shown in Figure 3a, the FACS profiles of H6O5-derived xenograft tumors were almost identical to those of primary Her2 tumors, demonstrating that the primary H6O5 line is a suitable cell model for studying Her2-induced primary mammary gland tumors. Among the FACS profiles of *in vitro* cultured H6O5 cells, only CD49f/CD61, ESA/CD61 and ESA/CD49f were akin to those in xenograft and primary tumors (Figure 3a). The differences in CD24/CD61 and CD24/CD49f profiles between *in vitro* cultured tumor cells and *in vivo* tumors might be attributable to *in vitro* culture condition. For identifying both *in vitro* and *in vivo* TICs, CD49f, CD61 and ESA are suitable markers for further studies. However, because of very strong fluorescent staining of ESA in H6O5 cells, we preferred the CD49f/CD61 combination for the FACS gating in cell sorting analysis. To develop a promising FACS gating strategy, we used the CD49f/CD61 profile of NMuMG to set the quadrant threshold lines for defining three different subpopulations in H6O5 cells (Figure 3b). These three subsets, CD49f^{high}CD61^{high}, CD49f^{high}CD61^{low} and CD49f^{low}CD61^{low}, are 12–15%, 35–40% and 25–30%, respectively, of total cells. To investigate the relationship between these three gated populations and ESA/CD24 profiles, we performed four-color FACS analysis on H6O5 cells using antibodies against these four markers. As shown in Figure 3b, 89.9% of CD49f^{high}CD61^{high} subset cells overlapped CD24^{high}ESA^{high} compared with only 25.4% of CD49f^{low}CD61^{low} subset cells. A strong correlation between these four potential stem/progenitor cell markers suggests that tumor cell types in Her2/neu-induced mammary tumors are heterogeneous and may be organized like a hierarchy proposed in the CSC model. This phenomenon has also been confirmed using isolated *in vivo* tumor cells (data not shown).

To address whether CD49f and CD61 are useful markers for enriching TICs, we examined tumorsphere formation abilities of these sorted fractions. The CD49f^{high}CD61^{high} subpopulation exhibited the highest tumorsphere formation efficiency ($2.8\pm0.6\%$) compared with CD49f^{high}CD61^{low} and CD49f^{low}CD61^{low} populations displaying much lower efficiencies ($0.8\pm0.3\%$ and $0.3\pm0.1\%$, respectively; Figure 4a). The observed significant increase in tumorsphere formation ability indicates that TICs are enriched in the CD49f^{high}CD61^{high} subpopulation.

Given that tumorigenicity is one of the hallmarks of TICs, we assessed the tumorigenic potential of the sorted cells with *in vitro* clonogenic and *in vivo* transplantation assays. As shown in Figure 4b, CD49f^{high}CD61^{high} cells exhibited the highest clonogenic ability compared with other two subset cells. For *in vivo*

Figure 2 FACS analysis of CD49f, CD24, ESA and CD61 in normal mammary glands, MMTV-*Her2/neu* preneoplastic mammary glands and tumors. FACS analysis was performed to examine the protein expression of CD49f, CD24, ESA and CD61 on mammary glands of FVB/N mice, as well as *Her2/neu* transgenic mice and on primary mammary tumors arising in MMTV-*Her2/neu* transgenic mice. CD24 versus CD49f, as well as ESA versus CD49f, CD24 versus CD61 and CD49f versus CD61 are shown in **a**–**c**, respectively. Histogram analyses of CD49f and CD61 are shown in the bottom panels of subfigure **a** and **b**, respectively. FVB/N-M, control mammary gland; HER2-M, *Her2/neu* transgenic mouse mammary gland; NER2-T, Her2/neu tumor.

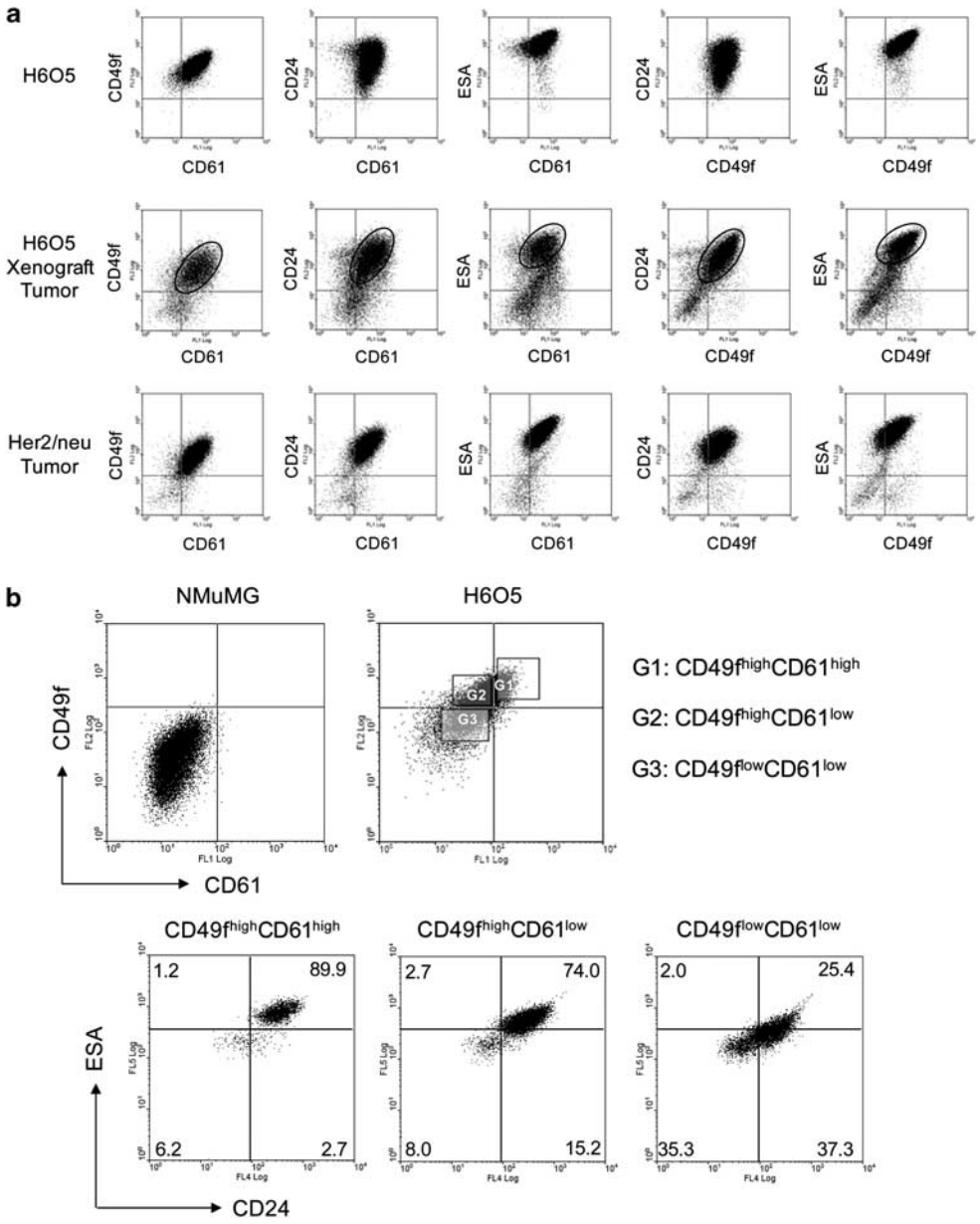

Figure 3 FACS profiling analysis of *in vitro* and *in vivo* Her2-overexpressing mammary tumor cells. (**a**) FACS profiling of CD49f, CD61, CD24 and ESA in *in vitro* cultured H6O5 cells, *in vivo* H6O5-derived xenograft tumors and primary Her2-induced mammary tumors. Isolated tumor cells were stained with several different combinations of antibodies against two surface antigens as indicated for two-color FACS analysis. The areas of two-color cell staining patterns in dot plot analysis of H6O5-derived xenograft tumors corresponding to those of primary Her2/neu tumors are circled. (**b**) FACS analysis of CD24 and ESA in gated CD49f^{high}CD61^{high}, CD49f^{high}CD61^{low} and CD49f^{low}CD61^{low} H6O5 cells. H6O5 cells were stained with CD61–fluorescein isothiocyanate, CD49f–phycoerythrin, CD24–allophycocyanin and ESA–allophycocyanin-cyanine 7 antibodies for four-color FACS analysis. The FACS profile of CD49f and CD61 in NMuMG cells was used to set the quadrant lines for defining high and low intensities of CD49f and CD61 in H6O5 cells.

transplantation assays, we transplanted serially diluted sorted subset cells from H6O5 or primary tumors, ranging from 5000 to 20, into syngeneic mice. For primary tumors, Lin$^-$CD49f^{high}CD61^{high} subset cells showed the highest TIC frequency (1/70) compared with other two subset cells showing much lower TIC frequencies (1/239 for Lin$^-$CD49f^{high}CD61^{low} and 1/1234 for Lin$^-$CD49f^{low}CD61^{low}; Table 1). The sorted cells from H6O5 manifested a similar trend of TIC frequencies (Table 1). Therefore, TICs in MMTV-*Her2/neu* mammary tumors or in H6O5 cells were significantly enriched in the CD49f^{high}CD61^{high} population. In addition to the highest frequency of TICs, the CD49f^{high}CD61^{high} subpopulation conferred an earliest onset of tumor formation compared with other two populations (Figure 4c). To address whether the CD49f^{high}CD61^{high} subpopulation possesses the drug-resistant characteristic of CSCs, clonogenic assays were performed on sorted CD49f^{high}CD61^{high} and CD49f^{low} CD61^{low} H6O5 cells treated with pacitaxel or doxorubicin.

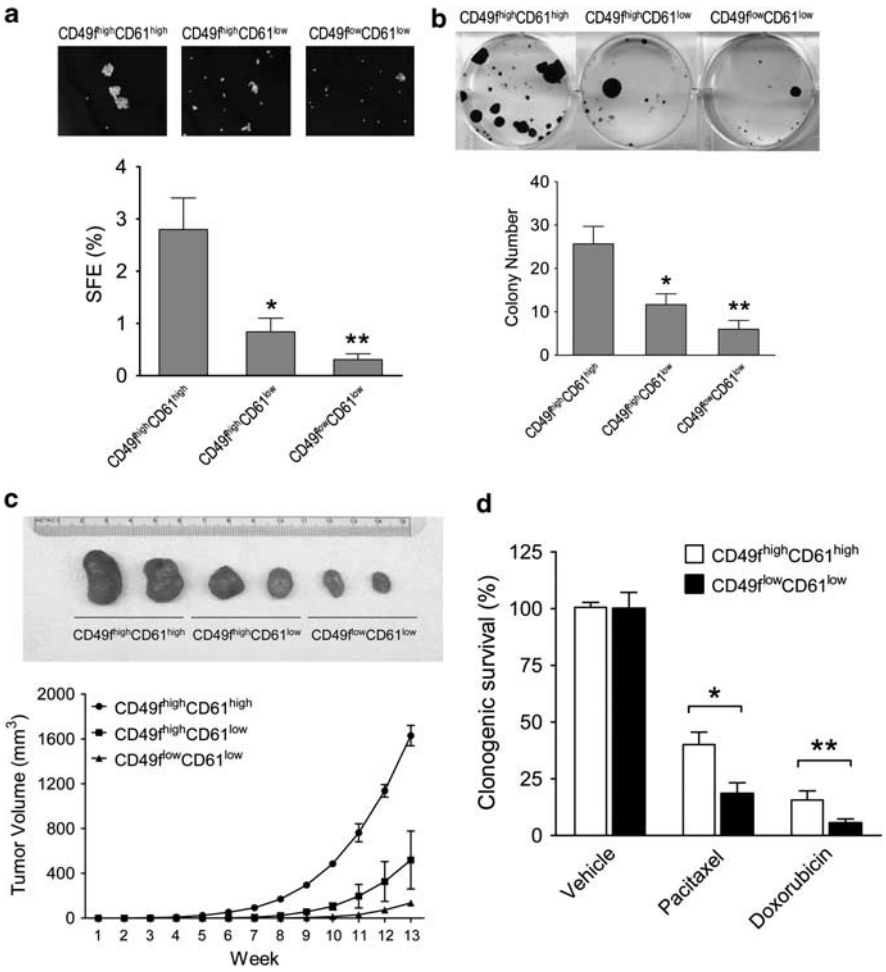

Figure 4 Isolated CD49f^{high}CD61^{high} cells exhibit features of TICs. (**a**) Enhanced tumorsphere formation ability of CD49f^{high}CD61^{high} cells. Sorted H6O5 cells were cultured in serum-free medium for sphere formation efficiency assays (SFE). (**b**) Increased clonogenic ability of CD49f^{high}CD61^{high} cells. A total of 1000 sorted H6O5 cells were seeded for clonogenic analysis. Bar graphs (the bottom panel) shown in **a** and **b** were generated from triplicate experiments. Error bars indicate s.d. *, **$P<0.05$ indicates statistically significant differences in sphere (**a**) or colony (**b**) numbers of the other two sorted fractions compared with that of the CD49f^{high}CD61^{high} fraction. (**c**) CD49f^{high}CD61^{high} cells showed the early onset of *in vivo* tumor formation. A total of 5000 sorted H6O5 cells were transplanted into the mammary glands of syngeneic mice. The tumor formation was monitored for 13 weeks, and then mice were killed and dissected. The dissected tumors were photographed and shown in the top panel. (**d**) CD49f^{high}CD61^{high} cells manifest drug resistance to pacitaxel and doxorubicin. Sorted H6O5 cells were treated with pacitaxel (2 nM) for 24 h and doxorubicin (25 ng/ml) for 10 h, and then 5000 drug-treated cells were plated in a 6-cm cell culture dish for clonogenic assays. Two weeks later, cell colonies were stained with crystal violet and colony numbers were counted for determining the percentages of clonogenic survival (drug-treated cells relative to vehicle-treated cells). The mean and s.d. of each drug-treated cell survival data set were derived from triplicate experiments. *, **$P<0.05$ indicates a statistically significant difference in clonogenic survival percentages of drug-treated CD49f^{high}CD61^{high} cells compared with those of drug-treated CD49f^{low}CD61^{low} cells.

Indeed, CD49f^{high}CD61^{high} cells were more resistant to these chemotherapeutic agents than CD49f^{low}CD61^{low} cells (Figure 4d).

CSCs are endowed with the ability to self-renew indefinitely and differentiate into phenotypically diverse cells. To reveal whether the CD49f^{high}CD61^{high} subpopulation exhibits these CSC features, we analyzed cellular subtypes in xenograft tumors derived from these three sorted cell fractions. The tumors derived from the CD49f^{high}CD61^{high} subpopulation were composed of cell populations similar to the original primary tumors, demonstrating that the CD49f^{high}CD61^{high} subpopulation is able to self-renew its own population ($12.2\pm0.7\%$) and also convert into other cell populations during tumor formation (Figure 5). In contrast, the tumors derived from CD49f^{high}CD61^{low} and CD49f^{low}CD61^{low} fractions contained significantly lower percentages of the CD49f^{high}CD61^{high} subpopulation ($7.9\pm0.6\%$ and $1.6\pm0.6\%$, respectively; Figure 5), indicating that these two sorted cell fractions contain less CSCs than the CD49f^{high}CD61^{high} fraction. These results show that CD49f^{high}CD61^{high} cells exhibit CSC traits of self-renewal and regeneration of heterogeneity of primary tumors.

Table 1 Frequency of TICs after transplantation of sorted H6O5 cells or primary mammary tumor cells into syngeneic mice

Injected cell number	*5000*	*1000*	*100*	*50*	*20*	*Frequency (TIC/cells)*
Sorted H6O5 cells						
$CD49f^{high}CD61^{high}$	2/2	2/2	3/4	1/4	1/4	1/62
$CD49f^{high}CD61^{low}$	2/2	2/2	1/4	0/4	0/4	1/176
$CD49f^{low}CD61^{low}$	2/2	2/2	0/4	0/4	0/4	NA
Sorted primary tumor cells						
$Lin^{-}CD49f^{high}CD61^{high}$	4/4	4/4	5/6	3/6	NA	1/70
$Lin^{-}CD49f^{high}CD61^{low}$	4/4	4/4	1/6	0/6	NA	1/239
$Lin^{-}CD49f^{low}CD61^{low}$	4/4	2/4	0/6	0/6	NA	1/1234

Abbreviations: NA, not available, TIC, tumor-initiating cell.

The TGFβ signaling and expression of EMT genes are specifically activated in the $CD49f^{high}CD61^{high}$ subpopulation

To further characterize TICs in Her2/neu tumors, gene expression profiling analysis was performed to examine expression of putative stem cell and differentiation marker genes. The CSC markers Abcg2 (Ishikawa and Nakagawa, 2009), Aldh1 (Ginestier *et al*., 2007), CD133 (Wright *et al*., 2008), Gli1 (Liu *et al*., 2006) and Tp63 (Hanker *et al*., 2010) were highly expressed in the $CD49f^{high}CD61^{high}$ subpopulation compared with other two sorted subpopulations (Figure 6a). In contrast, the expression levels of differentiation marker genes such as *Krt5*, *Krt6*, *Krt14* and *Krt18* were lowest in $CD49f^{high}CD61^{high}$ cells (Figure 6b). These data further confirm that the $CD49f^{high}CD61^{high}$ subpopulation is enriched for TICs with stem cell characteristics.

The TGFβ signaling has been known to have a critical role in regulating the pluripotency of human embryonic stem cells and CSCs via induction of an epithelial–mesenchymal transition (EMT; James *et al*., 2005; Mani *et al*., 2008). To examine the status of TGFβ signaling in sorted cells, we analyzed the expression of several selected TGFβ downstream responsive genes (*Pai*, *Il6*, *Igfbp3* and *Foxc2*). Compared with $CD49f^{low}CD61^{low}$ cells, expression of *Pai* (Yang *et al*., 2007), *Il6* (Park *et al*., 2003), *Igfbp3* (Kveiborg *et al*., 2001) and *Foxc2* (Mani *et al*., 2007) were upregulated in $CD49f^{high}CD61^{high}$ cells by 4.8-, 3.8-, 2.5- and 3.6-folds, respectively (Figure 6c). Moreover, increased phosphorylation and total levels of TGFβ downstream mediators Smad2/3 were observed in $CD49f^{high}CD61^{high}$ cells compared with $CD49f^{low}CD61^{low}$ cells (Figure 6d). Therefore, both gene expression and protein analysis data indicate that the TGFβ signaling was further activated in the TIC-enriched subpopulation. This suggests that the TGFβ signaling may have a critical role in Her2-mediated tumorigenesis and maintenance of the TIC population.

To investigate whether expression of the EMT genes in $CD49f^{high}CD61^{high}$ cells is upregulated concurrently with the TGFβ-target genes, we examined the expression status of five canonical EMT genes including *Cdh2*, *Sma*, *Snail*, *Twist1* and *Zeb1* (Kalluri and Weinberg, 2009). All of these genes were expressed in $CD49f^{high}CD61^{high}$ cells at the highest levels compared with other two subpopulations (Figure 6c). In addition, *Foxc2* analyzed as a TGFβ-target gene is also involved in EMT (Mani *et al*., 2007). These data show that $CD49f^{high}CD61^{high}$ cells express the highest TGFβ signaling and EMT gene signatures compared with non-TIC-enriched subsets.

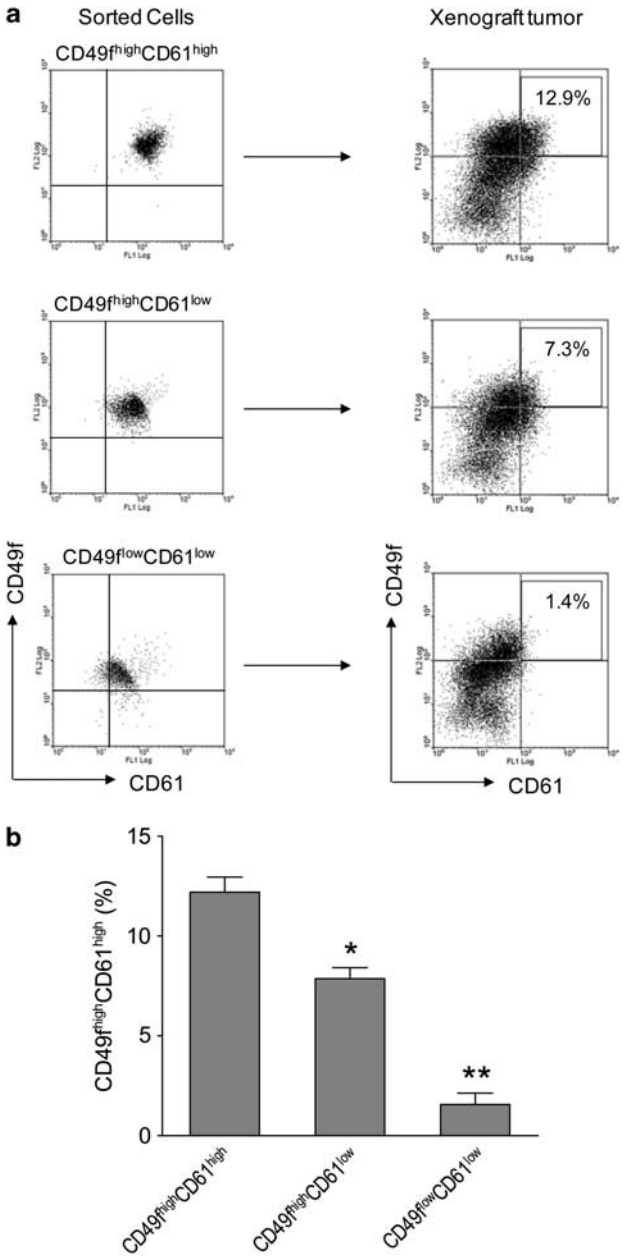

Figure 5 Repopulation of $CD49f^{high}CD61^{high}$ H6O5 cells during the development of xenograft tumors. (**a**) FACS analysis of CD49f and CD61 was performed on isolated $CD49f^{high}CD61^{high}$, $CD49f^{high}CD61^{low}$ and $CD49f^{low}CD61^{low}$ H6O5 cells, as well as their respective xenograft tumors. $CD49f^{high}CD61^{high}$ cells in xenograft tumors are boxed and their percentage is indicated in the box. (**b**) FACS data in **a** from triplicate transplantation experiments were plotted as a bar graph with error bars (indicating s.d.). *, $^{**}P<0.05$ indicates a statistically significant difference in $CD49f^{high}CD61^{high}$ percentages.

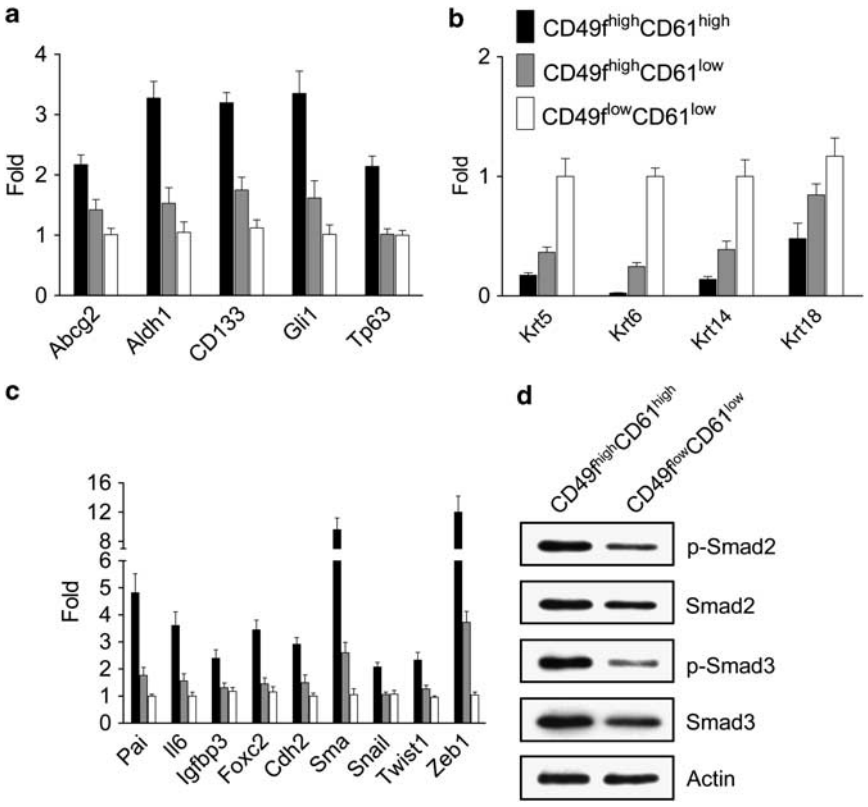

Figure 6 Isolated CD49f^{high}CD61^{high} cells display the stemness, TGFβ signaling and EMT gene signatures. Quantitative reverse transcriptase PCR analyses of stem cell (**a**), differentiation (**b**) and TGFβ/EMT (**c**) marker genes were performed on isolated CD49f^{high}CD61^{high}, CD49f^{high}CD61^{low} and CD49f^{low}CD61^{low} H6O5 cells. The mean and s.d. of each gene expression data were derived from triplicate experiments. (**d**) Enhanced activation of the TGFβ signaling pathway in sorted CD49f^{high}CD61^{high} cells compared with sorted CD49f^{low}CD61^{low} cells. Western blot analysis of phospho-Smad2 (Ser465/467), total Smad2, phospho-Smad3 (Ser423/425), total Smad3 and actin was performed on protein lysates derived from sorted CD49f^{high}CD61^{high} and CD49f^{low}CD61^{low} cells.

Treatment with TGFβ pathway inhibitors suppresses EMT gene expression and concurrently leads to a reduction in the TIC population

To examine the functional relevance of the TGFβ signaling in maintenance of the CD49f^{high}CD61^{high} population, we treated H6O5 cells with two different TGFβ-receptor-specific inhibitors, SB431542 and A-83-01. As shown in Figure 7a, these two inhibitors dramatically decreased the CD49f^{high}CD61^{high} subpopulation by over 70%. This effect was not due to inhibition of overall cell growth (Supplementary Figure 2). Nevertheless, the TGFβ signaling pathway was significantly inhibited as shown by drastically reduced levels of phosphorylated Smad2/3 (Supplementary Figure 3). These data suggest that blockade of the TGFβ signaling pathway may preferentially inhibit the self-renewal of TICs.

TGFβ activity is known to induce an EMT, which can potentially generate cells with stem cell properties (Mani *et al*., 2008). We then addressed whether abrogation of the TGFβ signaling pathway can lead to suppression of EMT marker gene expression. As shown in Figure 7b (the bottom panel), expression levels of five out of six EMT genes (except *Twist1*) in drug-treated cells dramatically decreased compared with those in vehicle-treated cells. These changes in the EMT gene expression profiles correlated with reverse EMT-like morphological changes in drug-treated cells (Figure 7b, the top panel). These data suggest that the TGFβ receptor inhibitors may preferentially inhibit the expansion of the TIC population by suppressing expression of genes involved in EMT.

To further validate whether the TIC population is reduced by abrogation of the TGFβ signaling, we examined clonogenic and tumorsphere-forming abilities of drug-treated cells. Consistent with FACS results (Figure 7a), 46.1 and 60.5% suppressive extents of tumorsphere formation were observed in SB431542-treated and A-83-01-treated cells, respectively, relative to vehicle-treated cells (Figure 7c). Besides a decrease in tumorsphere number, a significant reduction in sizes of tumorspheres from drug-treated cells was observed (data not shown). Similarly, treatment with SB431542 and A-83-01 resulted in a dramatic reduction in colony formation by 76.8% and 81.9%, respectively (Figure 7d). These findings, taken together, indicate that the TGFβ signaling has an essential role in maintenance of the Her2-transformed TIC population.

Suppression of the integrin-β3 pathway impairs TGFβ signaling and self-renewal of TICs

The molecular mechanisms underlying elevated activation of TGFβ signaling in the TIC-enriched subpopula-

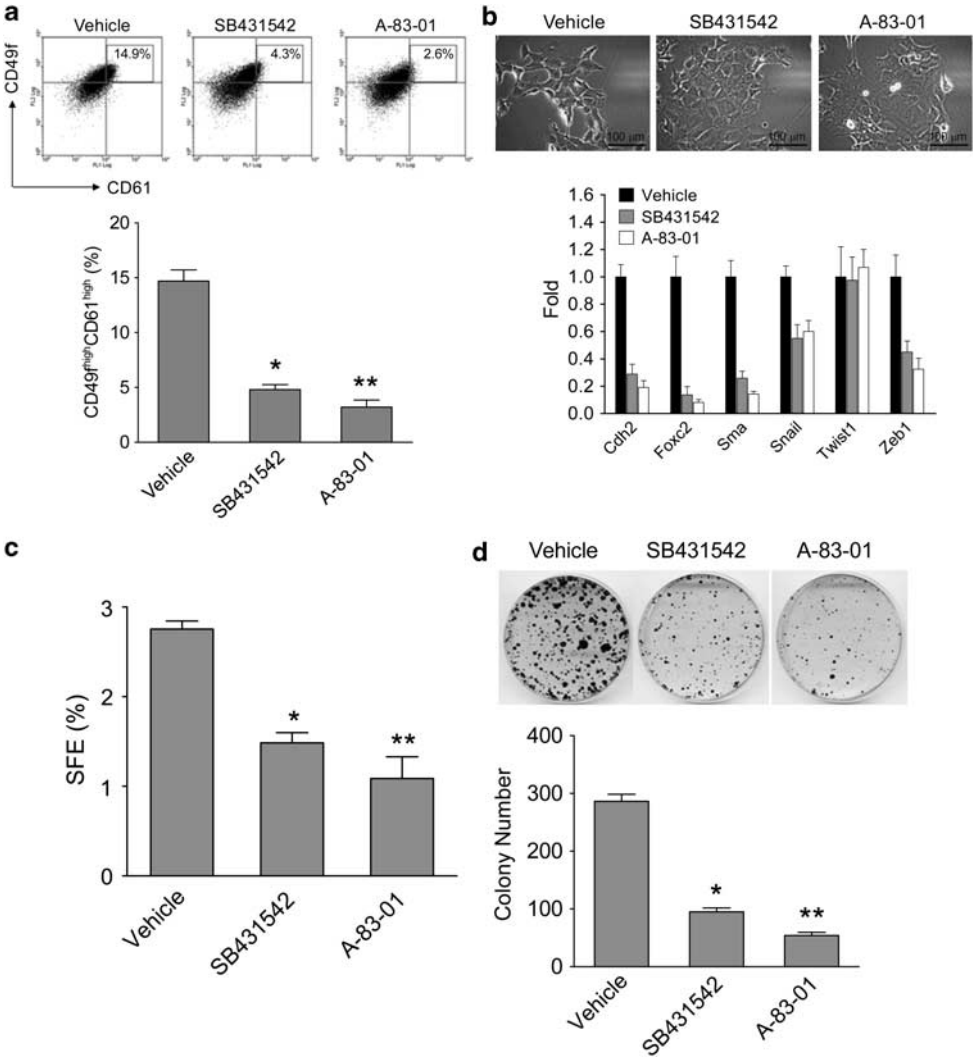

Figure 7 Inhibition of the TGFβ-receptor signaling leads to a decrease in TICs ($CD49f^{high}CD61^{high}$) cells, downregulation of EMT-programmed genes and abrogation of clonogenic and tumorsphere formation abilities of H6O5 cells. (**a**) FACS analysis of CD49f and CD61 in TGFβ inhibitor-treated H6O5 cells. $CD49f^{high}CD61^{high}$ cells are boxed and their percentage is indicated in the box. Results from triplicate experiments were plotted as a bar graph (the bottom panel). (**b**) Quantitative expression analysis of EMT-programmed genes in TGFβ inhibitor-treated H6O5 cells. Triplicate experiments were performed on H6O5 cells treated with TGFβ inhibitors as described in **a**. Microscopic photographs of vehicle- and drug-treated H6O5 cells are shown in the top panel. (**c**) Tumorsphere formation analysis of TGFβ inhibitor-treated H6O5 cells. Four-day-treated H6O5 cells were seeded for sphere formation assays. Triplicate experiments were performed. (**d**) Clonogenic analysis of TGFβ inhibitor-treated H6O5 cells. Stained colonies from vehicle- and drug-treated H6O5 cells are shown in the top panel. The bar graph (the bottom panel) was generated from triplicate experiments. Error bars represent s.d. *, **$P<0.05$ shown in **a**, **c** and **d** indicates a statistically significant difference.

tion are particularly interesting but unknown in our study. It has been shown that integrins are involved in activation of TGFβ signaling (Margadant and Sonnenberg, 2010). Given that the TIC-enriched subpopulation manifests the $CD49f^{high}CD61^{high}$ trait, it raises the possibility that these two integrin molecules may be implicated in activation of TGFβ signaling. Several lines of evidence have shown that αvβ3-integrin molecules are able to activate the TGFβ ligand *in vitro* and integrin-β3 interacts physically with the TGFβ receptor (TGF-βRII) to modulate the TGFβ signaling (Scaffidi *et al*., 2004; Galliher and Schiemann, 2006, 2007; Wipff *et al*., 2007). To unravel whether integrin-β3 (CD61) is engaged in activating TGFβ signaling in H6O5 cells, we performed small interfering RNA (siRNA) knockdown experiments on H6O5 cells. As shown in Figure 8a, siRNA-mediated knockdown of CD61 gave rise to decreased phosphorylation of FAK at Tyr397 and c-Src at Tyr416 (the downstream mediators of integrin-β3 signaling), indicating the downstream signaling of integrin β3 was inhibited by CD61 knockdown. Concurrent with reduced integrin-β3 signaling, the TGFβ signaling was attenuated by CD61 knockdown, indicated by decreased phosphorylation of Smad2/3 (Figure 8a). This result demonstrated that CD61 is required for activation of TGFβ signaling. We have shown that the TGFβ signaling is essential for maintenance of Her2-induced TICs (Figure 7). This suggests that CD61 may be crucial

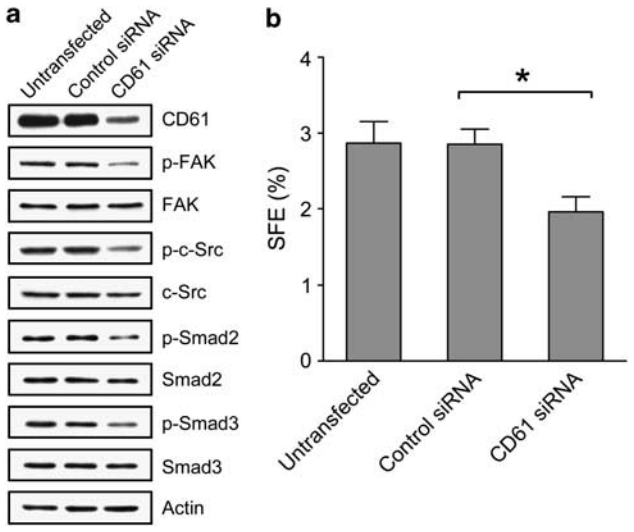

Figure 8 Knockdown of integrin-β3 (CD61) leads to a reduction in the TGFβ signaling and suppression of TIC self-renewal. (**a**) Western blot analysis of integrin-β3 and TGFβ signaling pathways in H6O5 cells with CD61 knockdown. H6O5 cells were transfected with control or CD61 siRNA, and transfected cells were harvested at 48 h after siRNA transfections for western blot analysis using antibodies against CD61, phospho-focal adhesion kinase (FAK) (Tyr397), total FAK, phospho-c-Src (Tyr416), total c-Src, phospho-Smad2 (Ser465/467), total Smad2, phospho-Smad3 (Ser423/425), total Smad3 and actin. Mouse CD61 siRNA is composed of a pool of four different CD61-specific siRNA duplexes (Dharmacon, Boulder, CO, USA). Untransfected H6O5 cells were also included in the parallel analysis. (**b**) Tumorsphere formation analysis of CD61-knockdown H6O5 cells. Sphere formation assays were performed on untransfected, control siRNA-transfected and CD61 siRNA-transfected H6O5 cells. $*P<0.05$ indicates a statistically significant difference.

for maintaining the TIC population. To test it, CD61 siRNA-transfected H6O5 cells were subjected to sphere formation assays compared with untransfected and control siRNA-transfected cells. A decrease of about 30% in sphere formation efficiency was observed in H6O5 cells with CD61 knockdown when compared with control cells (Figure 8b). These data, taken together, indicate that the cooperative integrin-β3–TGFβ signaling axis is mandatory for self-renewal ability of TICs.

Discussion

The growing consensus of the CSC model is attributable to the successful use of surface biomarkers for detecting and enriching CSCs in both human cancers and animal models (Clarke *et al*., 2006). However, the fact that no universal markers are able to identify TICs from all types of tumors may partially result from heterogeneous origins of cancer-initiating cells (Visvader, 2011). Although existence of TICs has been functionally identified in MMTV-*Her2/neu* tumors (Liu *et al*., 2007), no specific markers have been found to enrich them. In our study, combined analysis of CD24, CD49f and ESA revealed that MMTV-*Her2/neu*-induced mammary tumors are potentially derived from the aberrant mammary luminal progenitor cell population, which is based on these following lines of evidence: (1) The $CD24^{high}CD49f^{med/low}$ Ma-CFC progenitor population was anomalously expanded in preneoplastic MMTV-*Her2/neu* mammary glands relative to age-matched, normal counterparts (Figure 2a). (2) The detected, expanded cell population also displayed ESA^{high} (Figure 2a), a feature similar to human mammary luminal progenitor cells (Lim *et al*., 2009). (3) Gene expression profiles of MMTV-*Her2/neu* tumor cells are most concordant with the luminal progenitor gene signature (Lim *et al*., 2010). Therefore, we for the first time deciphered the potential cell population candidate for the origin of MMTV-*Her2/neu* mammary tumors. More importantly, we developed a method using the combination of CD49f and CD61 to identify and enrich TICs in MMTV-*Her2/neu* mammary tumors as well as in Her2-tumor-derived primary cell cultures.

Our data convincingly demonstrate that MMTV-*Her2/neu* tumors are heterogeneous and $CD49f^{high}$ $CD61^{high}$ subset cells are enriched for TICs based on both *in vitro* clonogenic and *in vivo* transplantation assays. It has been proposed by Vaillant *et al*. (2008) that MMTV-*Her2/neu* tumors are composed of a more homogeneous cell population according to FACS analysis. If tumors are composed of homogenous cells, we would expect that there is no correlated cellular distribution between markers, such as ESA, CD24, CD49f and CD61. In contrast to this expectation, the $CD49f^{high}CD61^{high}$ subset also showed highest expression levels of both CD24 and ESA than other subsets, indicating co-expression of these markers in a TIC-enriched subset of tumor cells. This notion is further supported by the fact that the stemness, TGFβ pathway and EMT gene signatures are specifically, highly expressed in the TIC-enriched subset. Taken together, our results suggest that the CSC model may be still applied to the Her2/neu-induced mouse tumor model.

Through enrichment of TICs in the $CD49f^{high}CD61^{high}$ subpopulation, we found that the TIC-enriched subpopulation expresses the highest levels of the TGFβ-responsive gene signature and exhibits increased TGFβ signaling compared with the other subpopulations of tumor cells. This suggests that cells with different phenotypes, even within the same tumor and tissue type, may differentially respond to TGFβ receptor inhibitors. Indeed, our results demonstrate that treatment with TGFβ receptor inhibitors had no effect on overall cell survival and growth but led to a specific reduction in the TIC population. Analogous to our findings, Shipitsin *et al*. (2007) found that the TGFβ signaling pathway is specifically activated in $CD44^+$ TICs, and treatment with the TGFβ receptor inhibitors had no significant effect on the proliferation and survival of tumor cells but resulted in dramatic morphological changes in $CD44^+$ cells, similar to mesenchymal–epithelial transition. Taken together, our and other studies further emphasize the importance of the TGFβ signaling for maintaining the pool of TICs in both mouse and human mammary tumors.

By knockdown of CD61, we have demonstrated that the integrin-β3 signaling pathway is imperative for

sustaining the TGFβ signaling, and the cooperative integrin-β3–TGFβ signaling axis has an indispensable role in maintaining Her2-transformed TICs. These findings for the first time provide novel evidence to link the integrin-β3–TGFβ signaling mode to TICs and to decipher, at least in part, the mechanisms underlying increased activation of TGFβ signaling in TICs. The αvβ3-integrin–Src signaling axis has been shown to facilitate TGFβ-mediated induction of EMT in mammary epithelial cells and promote breast cancer cell proliferation and invasion (Galliher and Schiemann, 2006, 2007). The oncogenic roles of the αvβ3-integrin–Src signaling axis in TGFβ signaling and EMT may account for our observations that the TIC-enriched $CD49f^{high}CD61^{high}$ subset exhibited increased TGFβ signaling and the typical EMT gene signature. According to accumulating evidence to show the importance of targeting of TICs in cancer therapy, our novel findings linking the integrin-β3–TGFβ signaling axis to Her2-transformed TICs may have immediate therapeutic implications due to the current testing of TGFβ pathway inhibitors and αvβ3-integrin antagonists in clinical trials (Biswas *et al*., 2006; Desgrosellier and Cheresh, 2010).

Materials and methods

Cell isolation and culture
Isolation of cancer epithelial cells from mammary tumors of MMTV-*Her2/neu* transgenic mice and establishment of the primary Her2-overexpressing tumor cell line H6O5 were described previously (Chen *et al*., 2010). The procedures for isolating Lin^- epithelial cells from mammary glands are described in the Supplementary Materials and methods.

Flow cytometry analysis and sorting
FACS analysis was performed using an FC500 CXP flow cytometer (Beckman Coulter, Fullerton, CA, USA). Cells were stained with the following antibodies: FITC- and PE-conjugated anti-CD49f (Becton Dickinson, Sparks, MD, USA), Alexa 488-conjugated anti-CD61 (BioLegend, San Diego, CA, USA), PE- and APC-conjugated anti-CD24 (BioLegend) and PE- and APC-Cy7-conjugated anti-ESA (BioLegend). Cell sorting was carried out on a FACSAria II cell sorter (Becton Dickinson).

In vitro *clonogenic assays*
Sorted or drug-treated H6O5 cells were plated in six-well plates at a density of 1000 cells per well or in 6-cm culture dishes at a density of 5000 cells/dish in complete medium. After 2 weeks, colonies were fixed and then stained with 0.1% crystal violet. Colonies with sizes $\geqslant 1$ mm were counted.

In vitro *tumorsphere formation assays*
Sorted or drug-treated viable H6O5 cells were plated in ultra-low attachment six-well plates (Corning, Acton, MA, USA) at a density of 10 000 cells/ml in serum-free DMEM/F12 medium (Invitrogen, Carlsbad, CA, USA) supplemented with 20 ng/ml epidermal growth factor (Sigma, St Louis, MO, USA), 10 ng/ml basic fibroblast growth factor (Sigma), 5 μg/ml insulin (Sigma), 1 × B27 supplement (Invitrogen) and 0.4% bovine serum albumin (Sigma). Cells were cultured under 5% CO_2 at 37 °C for a week (Gu *et al*., 2011).

In vivo *tumorigenesis assays*
Sorted cells were resuspended in 20 μl Dulbecco's modified Eagle's medium/F12 medium and mixed with 20 μl Matrigel (Becton Dickinson) at a 1:1 ratio and held on ice. The entire 40 μl sample was injected into either no. 3 or 4 mammary glands of MMTV-*Her2/neu* transgenic mice anesthetized with isoflurane according to the animal protocol approved by the University of South Carolina committee for research in vertebrate animals. Tumor sizes were measured weekly. Incidence of xenograft tumor formation was scored 12–13 weeks after injection.

Please see Supplementary Materials and methods for the description of cell isolation, quantitative real-time reverse transcriptase PCR, western blot, cell proliferation, siRNA transfection and statistical analyses.

Conflict of interest

The authors declare no conflict of interest.

Acknowledgements

We thank Dr Marai M Pena, Celestia Davis, Sara Johnson and Andrea Daamen for experimental assistance. This work was supported by the Elsa U Pardee Cancer Foundation grant (B94AFFAA), the American Cancer Society Research Award (RSG-10-067-01-TBE) to HC and NIH grant (3P20RR017698-08) to HC and QW.

References

Asselin-Labat ML, Sutherland KD, Barker H, Thomas R, Shackleton M, Forrest NC *et al*. (2007). Gata-3 is an essential regulator of mammary-gland morphogenesis and luminal-cell differentiation. *Nat Cell Biol* **9**: 201–209.

Biswas S, Criswell TL, Wang SE, Arteaga CL. (2006). Inhibition of transforming growth factor-beta signaling in human cancer: targeting a tumor suppressor network as a therapeutic strategy. *Clin Cancer Res* **12**: 4142–4146.

Chen H, Pimienta G, Gu Y, Sun X, Hu J, Kim MS *et al*. (2010). Proteomic characterization of Her2/neu-overexpressing breast cancer cells. *Proteomics* **10**: 3800–3810.

Cicalese A, Bonizzi G, Pasi CE, Faretta M, Ronzoni S, Giulini B *et al*. (2009). The tumor suppressor p53 regulates polarity of self-renewing divisions in mammary stem cells. *Cell* **138**: 1083–1095.

Clarke MF, Dick JE, Dirks PB, Eaves CJ, Jamieson CH, Jones DL *et al*. (2006). Cancer stem cells—perspectives on current status and future directions: AACR Workshop on cancer stem cells. *Cancer Res* **66**: 9339–9344.

Desgrosellier JS, Cheresh DA. (2010). Integrins in cancer: biological implications and therapeutic opportunities. *Nat Rev Cancer* **10**: 9–22.

Galliher AJ, Schiemann WP. (2006). Beta3 integrin and Src facilitate transforming growth factor-beta mediated induction of epithelial-mesenchymal transition in mammary epithelial cells. *Breast Cancer Res* **8**: R42.

Galliher AJ, Schiemann WP. (2007). Src phosphorylates Tyr284 in TGF-beta type II receptor and regulates TGF-beta stimulation of p38 MAPK during breast cancer cell proliferation and invasion. *Cancer Res* **67**: 3752–3758.

Ginestier C, Hur MH, Charafe-Jauffret E, Monville F, Dutcher J, Brown M *et al*. (2007). ALDH1 is a marker of normal and malignant human mammary stem cells and a predictor of poor clinical outcome. *Cell Stem Cell* **1**: 555–567.

Gu Y, Fu J, Lo P, Wang S, Wang Q, Chen H. (2011). The effect of B27 supplement on promoting *in vitro* propagation of Her2/neu-transformed mammary tumorspheres. *J Biotech Res* **3**: 7–18.

Guy CT, Webster MA, Schaller M, Parsons TJ, Cardiff RD, Muller WJ. (1992). Expression of the neu protooncogene in the mammary epithelium of transgenic mice induces metastatic disease. *Proc Natl Acad Sci USA* **89**: 10578–10582.

Hanker L, Karn T, Ruckhaeberle E, Gaetje R, Solbach C, Schmidt M *et al*. (2010). Clinical relevance of the putative stem cell marker p63 in breast cancer. *Breast Cancer Res Treat* **122**: 765–775.

Hynes NE, Jaggi R, Kozma SC, Ball R, Muellener D, Wetherall NT *et al*. (1985). New acceptor cell for transfected genomic DNA: oncogene transfer into a mouse mammary epithelial cell line. *Mol Cell Biol* **5**: 268–272.

Ishikawa T, Nakagawa H. (2009). Human ABC transporter ABCG2 in cancer chemotherapy and pharmacogenomics. *J Exp Ther Oncol* **8**: 5–24.

James D, Levine AJ, Besser D, Hemmati-Brivanlou A. (2005). TGFbeta/activin/nodal signaling is necessary for the maintenance of pluripotency in human embryonic stem cells. *Development* **132**: 1273–1282.

Kalluri R, Weinberg RA. (2009). The basics of epithelial-mesenchymal transition. *J Clin Invest* **119**: 1420–1428.

Korkaya H, Paulson A, Iovino F, Wicha MS. (2008). HER2 regulates the mammary stem/progenitor cell population driving tumorigenesis and invasion. *Oncogene* **27**: 6120–6130.

Kveiborg M, Flyvbjerg A, Eriksen EF, Kassem M. (2001). Transforming growth factor-beta1 stimulates the production of insulin-like growth factor-I and insulin-like growth factor-binding protein-3 in human bone marrow stromal osteoblast progenitors. *J Endocrinol* **169**: 549–561.

Li X, Lewis MT, Huang J, Gutierrez C, Osborne CK, Wu MF *et al*. (2008). Intrinsic resistance of tumorigenic breast cancer cells to chemotherapy. *J Natl Cancer Inst* **100**: 672–679.

Lim E, Vaillant F, Wu D, Forrest NC, Pal B, Hart AH *et al*. (2009). Aberrant luminal progenitors as the candidate target population for basal tumor development in BRCA1 mutation carriers. *Nat Med* **15**: 907–913.

Lim E, Wu D, Pal B, Bouras T, Asselin-Labat ML, Vaillant F *et al*. (2010). Transcriptome analyses of mouse and human mammary cell subpopulations reveal multiple conserved genes and pathways. *Breast Cancer Res* **12**: R21.

Liu JC, Deng T, Lehal RS, Kim J, Zacksenhaus E. (2007). Identification of tumorsphere- and tumor-initiating cells in HER2/Neu-induced mammary tumors. *Cancer Res* **67**: 8671–8681.

Liu S, Dontu G, Mantle ID, Patel S, Ahn NS, Jackson KW *et al*. (2006). Hedgehog signaling and Bmi-1 regulate self-renewal of normal and malignant human mammary stem cells. *Cancer Res* **66**: 6063–6071.

Magnifico A, Albano L, Campaner S, Delia D, Castiglioni F, Gasparini P *et al*. (2009). Tumor-initiating cells of HER2-positive carcinoma cell lines express the highest oncoprotein levels and are sensitive to trastuzumab. *Clin Cancer Res* **15**: 2010–2021.

Mani SA, Guo W, Liao MJ, Eaton EN, Ayyanan A, Zhou AY *et al*. (2008). The epithelial-mesenchymal transition generates cells with properties of stem cells. *Cell* **133**: 704–715.

Mani SA, Yang J, Brooks M, Schwaninger G, Zhou A, Miura N *et al*. (2007). Mesenchyme Forkhead 1 (FOXC2) plays a key role in metastasis and is associated with aggressive basal-like breast cancers. *Proc Natl Acad Sci USA* **104**: 10069–10074.

Margadant C, Sonnenberg A. (2010). Integrin-TGF-beta crosstalk in fibrosis, cancer and wound healing. *EMBO Rep* **11**: 97–105.

Park JI, Lee MG, Cho K, Park BJ, Chae KS, Byun DS *et al*. (2003). Transforming growth factor-beta1 activates interleukin-6 expression in prostate cancer cells through the synergistic collaboration of the Smad2, p38-NF-kappaB, JNK, and Ras signaling pathways. *Oncogene* **22**: 4314–4332.

Scaffidi AK, Petrovic N, Moodley YP, Fogel-Petrovic M, Kroeger KM, Seeber RM *et al*. (2004). alpha(v)beta(3) Integrin interacts with the transforming growth factor beta (TGFbeta) type II receptor to potentiate the proliferative effects of TGFbeta1 in living human lung fibroblasts. *J Biol Chem* **279**: 37726–37733.

Shackleton M, Vaillant F, Simpson KJ, Stingl J, Smyth GK, Asselin-Labat ML *et al*. (2006). Generation of a functional mammary gland from a single stem cell. *Nature* **439**: 84–88.

Shipitsin M, Campbell LL, Argani P, Weremowicz S, Bloushtain-Qimron N, Yao J *et al*. (2007). Molecular definition of breast tumor heterogeneity. *Cancer Cell* **11**: 259–273.

Stingl J, Eirew P, Ricketson I, Shackleton M, Vaillant F, Choi D *et al*. (2006). Purification and unique properties of mammary epithelial stem cells. *Nature* **439**: 993–997.

Vaillant F, Asselin-Labat ML, Shackleton M, Forrest NC, Lindeman GJ, Visvader JE. (2008). The mammary progenitor marker CD61/beta3 integrin identifies cancer stem cells in mouse models of mammary tumorigenesis. *Cancer Res* **68**: 7711–7717.

Visvader JE. (2011). Cells of origin in cancer. *Nature* **469**: 314–322.

Welm B, Behbod F, Goodell MA, Rosen JM. (2003). Isolation and characterization of functional mammary gland stem cells. *Cell Prolif* **36**(Suppl 1): 17–32.

Wipff PJ, Rifkin DB, Meister JJ, Hinz B. (2007). Myofibroblast contraction activates latent TGF-beta1 from the extracellular matrix. *J Cell Biol* **179**: 1311–1323.

Wright MH, Calcagno AM, Salcido CD, Carlson MD, Ambudkar SV, Varticovski L. (2008). Brca1 breast tumors contain distinct CD44+/CD24− and CD133+ cells with cancer stem cell characteristics. *Breast Cancer Res* **10**: R10.

Yang C, Patel K, Harding P, Sorokin A, Glass II WF. (2007). Regulation of TGF-beta1/MAPK-mediated PAI-1 gene expression by the actin cytoskeleton in human mesangial cells. *Exp Cell Res* **313**: 1240–1250.

Supplementary Information accompanies the paper on the Oncogene website (http://www.nature.com/onc)